Structural analysis of the human cannabinoid receptor one carboxyl-terminus identifies two amphipathic helices

ARTICLE *in* BIOPOLYMERS · JULY 2009

Impact Factor: 2.39 · DOI: 10.1002/bip.21179 · Source: PubMed

6 AUTHORS, INCLUDING:

Kwang Ahn
University of Connecticut
18 PUBLICATIONS **259** CITATIONS
SEE PROFILE

Achani Yatawara
Dartmouth College
14 PUBLICATIONS **179** CITATIONS
SEE PROFILE

Debra A Kendall
University of Connecticut
102 PUBLICATIONS **2,828** CITATIONS
SEE PROFILE

Dale F Mierke
Dartmouth College
228 PUBLICATIONS **4,808** CITATIONS
SEE PROFILE

Published in final edited form as:
Biopolymers. 2009 July ; 91(7): 565–573. doi:10.1002/bip.21179.

Structural Analysis of the Human Cannabinoid Receptor One Carboxyl-Terminus Identifies Two Amphipathic Helices

Kwang H. Ahn[1], **Maria Pellegrini**[2], **Natia Tsomaia**[2,*], **Achani K. Yatawara**[2], **Debra A. Kendall**[1], and **Dale F. Mierke**[2]

1 *Department of Molecular and Cell Biology, University of Connecticut, Storrs, CT 06269*

2 *Department of Chemistry, Dartmouth College, Hanover, NH 03755*

Abstract

Recent research has implicated the C-terminus of G-protein coupled receptors in key events such as receptor activation and subsequent intracellular sorting, yet obtaining structural information of the entire C-tail has proven a formidable task. Here, a peptide corresponding to the full-length C-tail of the human CB1 receptor (residues 400–472) was expressed in *E.coli* and purified in a soluble form. Circular dichroism (CD) spectroscopy revealed that the peptide adopts an α-helical conformation in negatively charged and zwitterionic detergents (48–51% and 36–38%, respectively), whereas it exhibited the CD signature of unordered structure at low concentration in aqueous solution. Interestingly, 27% helicity was displayed at high peptide concentration suggesting that self-association induces helix formation in the absence of a membrane mimetic. NMR spectroscopy of the doubly labeled (^{15}N- and ^{13}C-) C-terminus in dodecylphosphocholine (DPC) identified two amphipathic α-helical domains. The first domain, S401-F412, corresponds to the helix 8 common to G protein-coupled receptors while the second domain, A440-M461, is a newly identified structural motif in the distal region of the carboxyl-terminus of the receptor. Molecular modeling of the C-tail in DPC indicates that both helices lie parallel to the plane of the membrane with their hydrophobic and hydrophilic faces poised for critical interactions.

Keywords

GPCR; cannabinoid receptor one; CB1 carboxyl-terminus; amphipathic α-helices

INTRODUCTION

Cannabinoid receptors are members of the class A G protein-coupled receptor (GPCR) family. In human, two cannabinoid receptors, the CB1 receptor and the CB2 receptor, have been identified including two splice variantsof CB1, CB1a, [1] and CB1b. [2] The CB1 receptor is predominantly expressed in brain where it seems to play a role in regulating analgesia, appetite stimulation, learning and memory, hypothermia through inhibition of adenylyl cyclase, modulation of calcium channels, and activation of mitogen-activated protein kinase (for a review, see Ref. 3). In contrast, the CB2 receptor resides primarily in peripheral tissue, including tissue associated with the immune system such as the spleen and tonsils, and is

Correspondence to: Dale F. Mierke; e-mail: E-mail: Dale.F.Mierke@dartmouth.edu.
Reviewing Editor: C. Bush
**Present address:* Biomeasure, Inc, 27 Maple Street, Milford, MA 01757, USA.

involved in cannabinoid-mediated immune responses. Cannabinoid receptors bind and are activated by Δ^9-tetrahydrocannabinol, derived from *Cannabis sativa*. Several endogenous cannabinoid receptor agonists have also been identified, such as anandamide (arachidonoylethanolamide), 2-arachidonoyl-glycerol, and 2-arachidonylglyceryl ether.

CB1 shares the structural characteristics of other GPCRs: an extracellular N-terminus that is glycosylated, seven transmembrane α-helices with intracellular and extracellular intervening loops, and an intracellular C-terminus. Many studies have highlighted the intracellular loops of GPCRs, including CB1,[4,5] because these are considered functional domains that impact signal transduction and receptor activity through interaction with G proteins. More recently however, there is growing interest in the structure and role of the C-terminus (C-tail) of the receptors. Although many regions of the C-tail remain structurally undefined, the first high resolution crystal structure of bovine rhodopsin revealed an additional small helical region termed helix 8 between TM7 and the palmitoylation sites at position 322 and 323.[6] The recent crystal structure of the β_2-adrenergic receptor confirmed the existence of this helical segment.[7,8] Nonetheless, it is difficult to obtain detailed structural analysis of the entire C-tail due to its flexibility in aqueous solution, the sequence variability among GPCR family members, and because it is especially hydrophobic, making classical experimental strategies challenging. In previous studies, a peptide fragment corresponding to only helix 8 of the rat CB1 C-tail induced GTPγS binding to G proteins and inhibited adenylyl cyclase, suggesting that the small peptide mimicked the receptor in G-protein activation selectively.[9,10] This peptide fragment was studied using circular dichroism (CD) and NMR spepctroscopy and found to adopt different secondary structural features depending on the surfactant present.[10–13]

Aside from helix 8, there is very little structural information available for the C-termini of GPCRs. Sequence comparisons reveal great variation in the length and sequences of this region relative to the transmembrane domains. Indeed, a comparative analysis of the sequences of 199 GPCR C-termini reveals a broad range in length from 3 to 371 residues.[14] For instance, the β_2-adrenergic receptor C-tail is approximately twice the length of that of rhodopsin. Under crystallization conditions, the 85-residue segment of the β_2-adrenergic receptor was sufficiently flexible that the size and uniformity of the crystals were affected and only a truncated version of the receptor could be used to obtain structural data.[15] This disordered structure may reflect conformational plasticity and contribute to specificity for a variety of distinct biological roles.

The role(s) of the C-tail in the biogenesis and function of GPCRs has yet to be elucidated in detail. However, the presence of sequence features such as transmembrane interaction sites, palmiltoylation sites, phosphorylation sites, and PDZ-binding domains suggests that the C-tail may be critical for the regulation of receptor localization and activity. Indeed, mutational studies involving these domains revealed that the C-tail is critical for G-protein coupling,[16,17] modulating cell surface expression,[18,19] displaying an ER export signal,[20–22] postendocytic sorting,[23,24] dimerization,[25] and interacting with GPCR associating proteins, such as GEC1,[26,27] Drip78,[28] and CRIP1a.[29]

For CB1, it was reported that phosphorylation of serine and/or threonine residues in distinct regions of the C-tail regulate receptor internalization and desensitization.[30–32] In general, phosphorylation by different GPCR kinases is a critical step in both desensitization and internalization. The phosphoreceptor can uncouple G-proteins and recruit other proteins, such as arrestin, that are part of the cellular internalization machinery. However, the role of phosphorylation of particular residues in the C-tail of CB1 appears to be more complicated since the effect of phosphorylation on internalization is displayed in a cell-specific manner, suggesting the involvement of additional regulatory mechanisms.[32] Moreover, this complex set of activities is thought to include sites that extend well beyond helix 8.

To elucidate correlations in the structure and function of the CB1 C-tail, it is imperative that we develop a feasible strategy for obtaining structural information for the entire region. Here, we report for the first time the expression and purification of the complete 73-residue C-terminus of human CB1 in a soluble form. Secondary structural analysis using CD spectroscopy reveals a high degree of helicity in negatively charged and zwitterionic detergents. Consistent with the CD measurements, NMR spectroscopy of the full-length C-tail in dodecylphosphocholine (DPC) reveals about 38% helix, and defines two amphiphathic helices. Molecular dynamics (MD) simulations suggest that these are in close association with the membrane and poised to interact with proteins important for the regulation of receptor activity.

RESULTS

CB1 C-Terminus Expression and Purification

The sequence of the C-terminus of CB1 is shown in Figure 1A. The corresponding peptide was generated by expression in *E. coli* as a glutathione S-transferase (GST) fusion with a His-tag. Although hydropathy analysis[33] suggests that it is not especially hydrophobic, we found that inclusion of two lysine residues following the C-tail sequence and amino terminal to the His-tag was needed to enhance solubility of the peptide at high concentration. This strategy, developed by Deber and coworkers, has been found to have little impact on peptide structure and membrane interactive properties.[34,35] Following nickel-nitrilotriacetic acid (Ni-NTA) and glutathione affinity chromatography, and cleavage and separation from GST, the C-tail peptide was >95% pure (Figure 1B) and the final product cross-reacted with His-tag and CB1 C-tail antisera (Figure 1C).

Circular Dichroism Spectroscopy

To determine if the purified C-tail possessed secondary structure in aqueous solution, CD spectra were taken of the peptide at various concentrations (Figure 2A). We observed unordered structure below 0.1 m*M* peptide, some α-helical content (19%) at peptide concentrations of 0.1–0.5 m*M*, and more substantial helical content (27%) at concentrations of 0.5–1.5 m*M* peptide. This trend suggests that self-association of the peptide in aqueous solution induces a transition that includes some helical structure. In contrast, the CD spectra for the peptide in 50 m*M* DPC showed little concentration dependence; considerable helical content (35–39%) was observed for peptide in the 0.05–1.5 m*M* range. However, due to the limitations of obtaining CD spectra in the 190–200 nm range at high peptide concentration, the C-tail at 1.1 and 1.5 m*M* gave a best fit with slightly reduced helical content.

Using 50 μM peptide, we examined the influence of different detergents on the secondary structure of the C-tail (Figure 3). The peptide exhibits unordered structure with a negative minimum at about 200 nm in aqueous solution and in *n*-dodecyl β-D maltoside (DDM), a nonionic detergent (Figure 3A). In contrast, the presence of the negatively charged detergents, sodium deoxycholate (DOC) (Figure 3B) and sodium dodecyl sulfate (SDS) (Figure 3C) yielded spectra with a positive peak in the 190–195 nm range, a negative peak at ~208, and a second broader negative peak at ~222 nm. Consistent with these CD signatures, we determined that the peptide exhibited high helical content over a range of detergent concentrations (48 and 51% helical content in 30 m*M* DOC and 100 m*M* SDS, respectively), and no dependence on the CMC of either detergent was found. However, the spectra of the peptide in DOC showed broadening of the 208-nm band that may reflect the bulky nature of this detergent and its low aggregation number. Interestingly, the CD spectra of the C-tail peptide in the zwitterionic detergent, DPC (Figure 3D), showed the signatures of unordered structure below (0.1 m*M* comparable to 0.5 m*M* DPC; data not shown) the detergent CMC (1.1 m*M*) and of helical structure (36–38%) above the CMC. Although monomeric SDS and DOC influence the C-tail structure, DPC micelles and thus a mimic of the membrane leaflet are needed to accomplish

this task. Collectively, these results indicate that the hydrophobic environment of the detergent is important for the C-tail peptide helical structure. Since the C-tail peptide was unordered in the cationic detergent, cetyltrimethylammoniumbromide (data not shown), and in the nonionic detergent, DDM, yet helical in the anionic detergents SDS and DOC as well as the zwitterionic detergent, DPC, electrostatic interactions must also play a role.

NMR Spectroscopy

The evidence of secondary structure in micelles provided by CD spectroscopy led us to use NMR to examine the three-dimensional structure, in the presence of 200 m*M* DPC, to provide a membrane-mimetic environment. The backbone resonances could be completely assigned for ~60% of the residues of the C-terminal construct. An additional 18 spin systems could be detected but gave rise to weak and sparse signals (at times severely overlapped with intense resonances), which prevented complete resonance assignment. This was particularly true for the C-terminal portion of the molecule, in which the available chemical shift data are consistent with an α-helix. It is worth noting that the sequence V442-V459 shows a high propensity to fold in an amphipathic helix from secondary structure prediction. The tight interaction of the amphipathic helix with the zwitterionic micelle is deemed responsible for the observed line-broadening. Based on the available assignments, the secondary shifts indicate that the C-terminus adopts two α-helices, from S401-F412 and A440-M461. The first helix, the so-called helix 8 of GPCRs, has been well described in the literature and observed in the X-ray structures of rhodopsin and β-adrenergic receptors, as well as in small peptides of this region.[11,13,15] This helix is very amphipathic and found to be perpendicular to the 7TM bundle, with the hydrophobic face projecting toward the membrane surface. The second newly identified helix, consisting of a 22 amino acid stretch for A440-M461 also presents an amphipathic helix, assumed to lie on the membrane surface. The remainder of the molecule is found to be unstructured based on the NMR data. These findings, accounting for 34 of 86 residues (39%) of the full-length construct are in an α-helix, fully consistent with the CD data.

Molecular Modeling

Placing the structural findings of the C-terminus into the receptor model is greatly assisted by the presence of helix 8 within the homology model templates for which X-ray structures are available (i.e., rhodopsin and β-adrenergic receptors). In Figure 4, the S401-F412 α-helix has been superimposed on helix 8 generated from these homology models, placing L404, F408, and F412 projecting upward toward the membrane surface. The opposite face of the helix is mostly charged consisting of D403, R405, and R409. Given the large intervening sequence of unstructured protein, consisting of ~28 residues, we have chosen to leave the exact location of the second α-helix undefined (Figure 4). Based on the amphipathic nature of this helix (Figure 5) and the NMR line-broadening indicating association with the micelle, we assume the helix to be lying on the inner-membrane surface, perpendicular to the 7TM helical bundle.

To further examine the possible orientations and relative topological arrangement of these two α-helices with respect to TM7, we carried out a MD simulation of the C-terminus attached to TM7 [consisting of human CB1 (374–472)] fully solvated in a lipid bilayer. The results of this 150-ps MD simulation clearly demonstrate the energetic stability of the two helices to lie on the membrane surface. The intervening residues between the two helices are flexible, and found to fluctuate during the simulation. Interestingly, the distance between the end of helix 8 (residue F412) and the beginning of the second helix (residue 440) is rather stable (although with small fluctuations) at 26 Å. A snap shot from this simulation is illustrated in Figure 6.

DISCUSSION

The carboxyl-terminal tail of the CB1 receptor is important for receptor activation, desensitization, and intracellular sorting during internalization. It has been implicated as a site for interaction with G proteins,[9,10,36] CRIP 1a,[29] protein kinases,[31] arrestins,[37] and with itself or other receptors to form dimers.[38–40] Here, we have successfully purified the entire 73-residue C-tail of the receptor for spectroscopic characterization to elucidate structural domains, and possible membrane and/or protein interaction sites, within this region of the receptor.

The CD spectra of the entire C-terminus indicate that it has the propensity to adopt a highly helical structure when presented with a hydrophobic surface that can be contributed either by induction of amphipathic helices in neighboring peptides or detergent. In aqueous solution, helicity is dependent on peptide concentration, consistent with self-association to sequester the hydrophobic faces of amphipathic helices. In negatively charged and zwitterionic detergents, the detergent provides the hydrophobic surface for interaction so helix formation is not peptide-concentration dependent.

Our findings based on the incorporation of ^{15}N and ^{13}C in the full C-tail for NMR analysis, indicate that the helix content is attributed to the formation of two helical domains in the presence of zwitterionic micelles composed of DPC. Molecular modeling indicates that these two helices lie on the membrane surface, yet the lack of additional structural elements in the NMR spectra, indeed of a tertiary fold, limits the ability to map the relative and topological orientation of these domains further. Similar results have been reported for the C-terminus of the bradykinin receptor, in which the C-terminus was observed to adopt three α-helices, all associated with the membrane surface.[41]

Importantly, our experiments identify the specific amino acids of these helical domains (S401-F412 and A440-M461) and reveal the strong amphipathic nature of each. Since we have used the entire human CB1 C-terminus, assignment of the beginning and end of each helical segment within the polypeptide is less prone to the challenges of the floppy ends of shorter peptides and possible changes in helical content. The strong association of these helices with the membrane surface, largely provided by the hydrophobic face of each helix, stabilizes these helical domains for interaction with other proteins involved in the receptor function. The polar face of each helix, not only enriched in charged residues, but also including some hydroxyl-containing serines and threonines, projects into the cytosol. Indeed, given that many of the proteins interacting with GPCRs are membrane associated themselves, the interaction will be greatly facilitated by being limited to the two-dimensional (2D) surface of the membrane. Similar models for the interaction of peptide ligands with the extracellular portions of GPCRs have been demonstrated.[42,43] The recent X-ray structure of squid rhodopsin also contains a second α-helix (helix 9) within the C-terminus.[44] This helix consists mainly of charged residues and is found to project away from the membrane surface, forming a number of contacts with the cytoplasmic helical extension of TM5, TM6, and IC3. The charged residues of helix 9 projecting out into the cytosol have been suggested as a point of contact with Gq.[45]

The membrane proximal helix 8 of the PAR1 receptor[46] and of the CB1 receptor[47] are thought to link via several non-covalent interactions to the NPXXY motif on helix 7 and TM1-IC1. This is consistent with a role for this helix in receptor activation and impacting G protein coupling. However, the more distal C-terminal domain also seems to be involved in signaling. Nie and Lewis[48] demonstrated that truncation of the human CB1 distal C-terminal domain (Δ418–472), which includes the second helix identified here, affected the magnitude and kinetics of Ca^{2+} current inhibition via G protein coupling, suggesting the possibility that this domain could directly, or indirectly through interaction with another protein, regulate

signaling. When CB1 with the same region deleted is expressed in Sf9 cells, the production level of the receptor is increased twofold and the basal activity enhanced relative to the wild-type receptor, also suggesting a regulatory function for this region.[49] Moreover, several of the serines and threonines of the region have been implicated as phosphorylation sites. The segment encompassing CB1 residues 418–439 (rat CB1) is critical for receptor desensitization but not internalization, while phosphorylation of residues within 460–473 (rat CB1) affect internalization.[30,31] Interestingly, a CB1 mutant with a deletion of only residues 460–473, that lie carboxy-terminal to the second helix identified here, is still internalized leaving open the possibility that the helix is involved. Although one study suggests that a peptide fragment corresponding to the unstructured region between the two helical motifs interacts with arrestin as part of the internalization process,[37] that study did not have the benefit of the identification of the helical domains assigned here and a longer peptide including the helix may enhance the interaction. In addition to providing possible sites for interaction with regulatory proteins, the amphipathic helices may provide hydrophobic surfaces for dimerization during the receptor life cycle. It has been reported that CB1 can form homodimers as well as heterodimers with the D2 dopamine receptor, opioid receptor, and orexin-1 receptor for cross-regulation of activity,[39,40,50] though it is not clear to what extent the C-terminus is involved. Future studies will be aimed at determining the role of each amphipathic helix in regulating signal transduction and receptor trafficking.

MATERIALS AND METHODS

Mutagenesis and Construction of the CB1 C-Terminal DNA Coding Region

The cDNA containing the coding region for the human CB1 C-terminus (73 residues) was subcloned into the BamHI and EcoRI sites of the *E. coli* GST gene fusion expression vector, pGEX-6P-1 (GE Healthcare). The DNA bases coding for a six-histidine tag (His-tag) were inserted between the last residue of the C-terminus and a stop codon using the QuikChange Site-Directed Mutagenesis Kit (Stratagene). Two lysine residues were also inserted between the C-terminal tail sequence and the His-tag to increase solubility during purification. The construct was confirmed by automated DNA sequencing (Beckman).

Peptide Expression and Purification

E. coli strain BL21(DE3) (Invitrogen), transformed with the CB1 C-tail, was grown in M9 minimal medium for CD experiments. For NMR spectroscopy, $^{15}NH_4Cl$ (Spectra Stable Isotopes) and ^{13}C-glucose (Supplier) were used. Four liters of M9 medium with ampicillin (250 μg/ml) were inoculated with the overnight culture and grown at 37°C until the OD_{600} reached 0.5. The culture was then induced with 0.5 m*M* isopropyl-β-thiogalactopyranoside for 6 h at 30°C. The cells were centrifuged at 6000*g* for 20 min and the pellet was resuspended in lysis buffer (50 m*M* NaH_2PO_4, 300 m*M* NaCl, 10 m*M* imidazole, pH 8.0, and 0.1 m*M* phenylmethylsulphonyl fluoride). The cells were lysed by sonication for 3 min at a power setting of 5 and a duty cycle of 50%. Triton X-100 was added to 1% (v/v) and the lysate was stirred at 4°C for 30 min, then centrifuged for 30 min at 22,500*g*. The supernatant was mixed with Ni-NTA agarose beads (Qiagen) for 1 h at 4°C and the resin subsequently washed with 50 m*M* NaH_2PO_4, 300 m*M* NaCl, and 20 m*M* imidazole, pH 8.0. His-tagged peptide was eluted with 50 m*M* NaH_2PO_4, 300 m*M* NaCl, and 250 m*M* imidazole, pH 8.0. The eluted sample was purified further using glutathione-Sepharose 4B (GE Healthcare), followed by PreScission protease (GE Healthcare) cleavage for 18 h at 4°C. The sample was then desalted and concentrated using a Centricon filter device (Millipore). The purity of the peptide was verified by SDS-PAGE and its identity confirmed via Western blot.

Circular Dichroism Spectroscopy

The CD spectra were measured on a Jasco J-715 CD spectrometer (Tokyo, Japan). Peptide concentrations were determined by amino acid analysis (Yale University Keck Biotechnology Resource Laboratory, New Haven, CT). Typically, the peptide concentration used was 50 μM except when the concentration-dependence of the secondary structure was analyzed as indicated. All spectra were corrected by subtraction of spectra for reference samples containing only buffer, detergents, or trifluoroethanol. The spectra were recorded using a 0.1-cm path length quartz cuvette from 250 to 190 nm at 20°C at a scan speed of 50 nm/min and a response time of 0.5 s. Four spectra were collected and averaged per sample. CD intensities are converted to mean residue molar ellipticity [θ], using the following equation: $[\theta] = \theta_{obs}/10lcn$ (in degree cm^2 $dmol^{-1}$), where θ_{obs} is the observed ellipticity in millidegrees, l is the path length in centimeters, c is the final concentration of the peptides in molarity, and n is number of amino acid residues. The CD spectra were analyzed to obtain quantitative estimations of the secondary structure using three different methods, CDSSTR, CONTINLL, and SELCON3 (CDPRO software). CONTINLL gave a best fit with the lowest root mean-square deviation (root mean square deviation) for the observed sample spectra and the derived combination of basis spectra, and is the method used for values reported in the text. The mean helix content was also calculated from mean residue molar ellipticity values at 222 nm using the following equation: % of α-helix = $100([\theta_{222}]/-39500(1-2.57/n))$, where n is the number of peptide bonds.

Nuclear Magnetic Resonance Spectroscopy

NMR spectra were recorded on a 2.1 mg/ml sample in 50 m*M* phosphate buffer, pH = 6.8 (95% H_2O, 5% D_2O), 50 m*M* NaCl, containing 200 m*M* DPC-d_{35}, at a temperature of 22°C. All data were acquired on a Bruker Avance 500 spectrometer equipped with a TCI cryogenic probe. A basic set of triple resonance experiments was utilized for backbone assignment: HNCA, HNCACB, CBCACONH, HNCO, HNCACO, and 3D ^{15}N-NOESY.

Molecular Modeling

The generation of the model of the CB1 receptor has been described in a previous publication.[51] The C-terminus of the CB1 receptor was built using a home-written distance geometry program with the structural features (two α helices) introduced by chiral volume constraints. The system was energy minimized using the Discover program (MSI) employing the cvff force field. The figures were generated using Chimera (USCF).

Molecular Dynamics of TM7-C-Terminus

The topological orientation of TM 7 and the C-terminus of CB1 protein on the membrane were generated using the *VMD* (version 1.8.6)[52] graphical interface. A POPC lipid bilayer of size 80 × 80 $Å^2$ was created using the membrane plugin within the program. The protein was inserted into the bilayer, followed by solvating the system, and neutralizing the membrane-protein system by adding necessary counter ions. The complete system (protein, lipid bilayer, water, counter ions) represented a total of 63,134 atoms. Molecular dynamic simulations were performed using *NAMD*, version 2.6.[53] Energy minimization was carried out for 25,000 steps followed by 150-ps run time for equilibration. The system was examined with NPT ensemble with constant membrane area using three-dimensional periodic boundary conditions. The temperature of the system was kept at ~300 K with Langevin dynamics and constant pressure was maintained at 1 atm using a Langevin-piston method. The Newtonian equations of motion were integrated using 2 fs time-step considering all bonds involving hydrogen were rigid. Long-range forces with a cut-off of 12 A Å and full-system electrostatic interactions were taken into account using the particle mesh Ewald approach. The system trajectories and extended system trajectories for the periodic cell parameters were recorded for every 1-ps runtime. The MD simulation was run for 150 ps on a multi-CPU cluster.

Acknowledgments

Contract grant sponsor: National Institutes of Health

Contract grant numbers: GM082054, DA018428, DA020763

References

1. Shire D, Carillon C, Kaghad M, Calandra B, Rinaldi-Carmona M, Le Fur G, Caput D, Ferrara P. J Biol Chem 1995;270:3726–3731. [PubMed: 7876112]
2. Ryberg E, Vu HK, Larsson N, Groblewski T, Hjorth S, Elebring T, Sjögren S, Greasley PJ. FEBS Lett 2005;579:259–264. [PubMed: 15620723]
3. Porter AC, Felder CC. Pharmacol Ther 2001;90:45–60. [PubMed: 11448725]
4. Ulfers AL, McMurry JL, Miller A, Wang L, Kendall DA, Mierke DF. Protein Sci 2002;11:2526–2531. [PubMed: 12237474]
5. Ulfers AL, McMurry JL, Kendall DA, Mierke DF. Biochemistry 2002;41:11344–11350. [PubMed: 12234176]
6. Palczewski K, Kumasaka T, Hori T, Behnke CA, Motoshima H, Fox BA, Le TI, Teller DC, Okada T, Stenkamp RE, Yamamoto M, Miyano M. Science 2000;289:739–745. [PubMed: 10926528]
7. Rosenbaum DM, Cherezov V, Hanson MA, Rasmussen SG, Thian FS, Kobilka TS, Choi HJ, Yao XJ, Weis WI, Stevens RC, Kobilka BK. Science 2007;318:1266–1273. [PubMed: 17962519]
8. Cherezov V, Rosenbaum DM, Hanson MA, Rasmussen SG, Thian FS, Kobilka TS, Choi HJ, Kuhn P, Weis WI, Kobilka BK, Stevens RC. Science 2007;318:1258–1265. [PubMed: 17962520]
9. Howlett AC, Song C, Berglund BA, Wilken GH, Pigg JJ. Mol Pharmacol 1998;53:504–510. [PubMed: 9495818]
10. Mukhopadhyay S, Cowsik SM, Lynn AM, Welsh WJ, Howlett AC. Biochemistry 1999;38:3447–3455. [PubMed: 10079092]
11. Choi G, Guo J, Makriyannis A. Biochim Biophys Acta 2005;1668:1–9. [PubMed: 15670725]
12. Xie XQ, Chen JZ. J Biol Chem 2005;280:3605–3612. [PubMed: 15550382]
13. Grace CR, Cowsik SM, Shim JY, Welsh WJ, Howlett AC. J Struct Biol 2007;159:359–368. [PubMed: 17524664]
14. Otaki JM, Firestein S. J Theor Biol 2001;211:77–100. [PubMed: 11419953]
15. Rasmussen SG, Choi HJ, Rosenbaum DM, Kobilka TS, Thian FS, Edwards PC, Burghammer M, Ratnala VR, Sanishvili R, Fischetti RF, Schertler GF, Weis WI, Kobilka BK. Nature 2007;450:383–387. [PubMed: 17952055]
16. Delos Santos NM, Gardner LA, White SW, Bahouth SW. J Biol Chem 2006;281:12896–12907. [PubMed: 16500896]
17. Grünewald S, Schupp BJ, Ikeda SR, Kuner R, Steigerwald F, Kornau HC, Köhr G. Mol Pharmacol 2002;61:1070–1080. [PubMed: 11961124]
18. Venkatesan S, Petrovic A, Locati M, Kim YO, Weissman D, Murphy PM. J Biol Chem 2001;276:40133–40145. [PubMed: 11514564]
19. Oksche A, Dehe M, Schülein R, Wiesner B, Rosenthal W. FEBS Lett 1998;424:57–62. [PubMed: 9537515]
20. Duvernay MT, Zhou F, Wu G. J Biol Chem 2004;279:30741–30750. [PubMed: 15123661]
21. Schülein R, Hermosilla R, Oksche A, Dehe M, Wiesner B, Krause G, Rosenthal W. Mol Pharmacol 1998;54:525–535. [PubMed: 9730911]
22. Robert J, Clauser E, Petit PX, Ventura MA. J Biol Chem 2005;280:2300–2308. [PubMed: 15528211]
23. Trejo J, Coughlin SR. J Biol Chem 1999;274:2216–2224. [PubMed: 9890984]
24. Delhaye M, Gravot A, Ayinde D, Niedergang F, Alizon M, Brelot A. Mol Pharmacol 2007;72:1497–1507. [PubMed: 17855654]
25. Cvejic S, Devi LA. J Biol Chem 1997;272:26959–26964. [PubMed: 9341132]
26. Wang H, Bedford FK, Brandon NJ, Moss SJ, Olsen RW. Nature 1999;397:69–72. [PubMed: 9892355]

27. Chen C, Li JG, Chen Y, Huang P, Wang Y, Liu-Chen LY. J Biol Chem 2006;281:7983–7993. [PubMed: 16431922]
28. Bermak JC, Li M, Bullock C, Zhou QY. Nat Cell Biol 2001;3:492–498. [PubMed: 11331877]
29. Niehaus JL, Liu Y, Wallis KT, Egertová M, Bhartur SG, Mukhopadhyay S, Shi S, He H, Selley DE, Howlett AC, Elphick MR, Lewis DL. Mol Pharmacol 2007;72:1557–1566. [PubMed: 17895407]
30. Hsieh C, Brown S, Derleth C, Mackie K. J Neurochem 1999;73:493–501. [PubMed: 10428044]
31. Jin W, Brown S, Roche JP, Hsieh C, Celver JP, Kovoor A, Chavkin C, Mackie K. J Neurosci 1999;19:3773–3780. [PubMed: 10234009]
32. Daigle TL, Kwok ML, Mackie K. J Neurochem 2008;106:70–82. [PubMed: 18331587]
33. Kyte J, Doolittle RF. J Mol Biol 1982;157:105–132. [PubMed: 7108955]
34. Liu LP, Deber CM. Biopolymers 1998;47:41–62. [PubMed: 9692326]
35. Melnyk RA, Partridge AW, Yip J, Wu Y, Goto NK, Deber CM. Biopolymers 2003;71:675–685. [PubMed: 14991677]
36. Mukhopadhyay S, McIntosh HH, Houston DB, Howlett AC. Mol Pharmacol 2000;57:162–170. [PubMed: 10617691]
37. Bakshi K, Mercier RW, Pavlopoulos S. FEBS Lett 2007;581:5009–5016. [PubMed: 17910957]
38. Mackie K. Life Sci 2005;77:1667. [PubMed: 15978631]
39. Kearn CS, Blake-Palmer K, Daniel E, Mackie K, Glass M. Mol Pharmacol 2005;67:1697–1704. [PubMed: 15710746]
40. Ellis J, Pediani JD, Canals M, Milasta S, Milligan G. J Biol Chem 2006;281:38812–38824. [PubMed: 17015451]
41. Piserchio A, Zelesky V, Yu J, Taylor L, Polgar P, Mierke DF. Biopolymers 2005;80:367–373. [PubMed: 15682437]
42. Lutz J, Romano-Götsch R, Escrieut C, Fourmy D, Mathä B, Müller G, Kessler H, Moroder L. Biopolymers 1997;41:799–817. [PubMed: 9128441]
43. Schwyzer R. Biopolymers 1995;37:5–16. [PubMed: 7880967]
44. Murakami M, Kouyama T. Nature 2008;453:363–367. [PubMed: 18480818]
45. Schertler GF. Nature 2008;453:292–293. [PubMed: 18480801]
46. Swift S, Leger AJ, Talavera J, Zhang L, Bohm A, Kuliopulos A. J Biol Chem 2006;281:4109–4116. [PubMed: 16354660]
47. Anavi-Goffer S, Fleischer D, Hurst DP, Lynch DL, Barnett-Norris J, Shi S, Lewis DL, Mukhopadhyay S, Howlett AC, Reggio PH, Abood ME. J Biol Chem 2007;282:25100–25113. [PubMed: 17595161]
48. Nie J, Lewis DL. Neuroscience 2001;107:161–167. [PubMed: 11744255]
49. Chillakuri CR, Reinhart C, Michel H. FEBS J 2007;274:6106–6115. [PubMed: 17986258]
50. Rios C, Gomes I, Devi LA. Br J Pharmacol 2006;148:387–395. [PubMed: 16682964]
51. D'Antona AM, Ahn KH, Wang L, Mierke DF, Lucas-Lenard J, Kendall DA. Brain Res 2006;1108:1–11. [PubMed: 16879811]
52. Humphrey W, Dalke A, Schulten K. J Mol Graph 1996;14:33–38. [PubMed: 8744570]
53. Phillips JC, Braun R, Wang W, Gumbart J, Tajkhorshid E, Villa E, Chipot C, Skeel RD, Kale L, Schulten K. J Comput Chem 2005;26:1781–1802. [PubMed: 16222654]

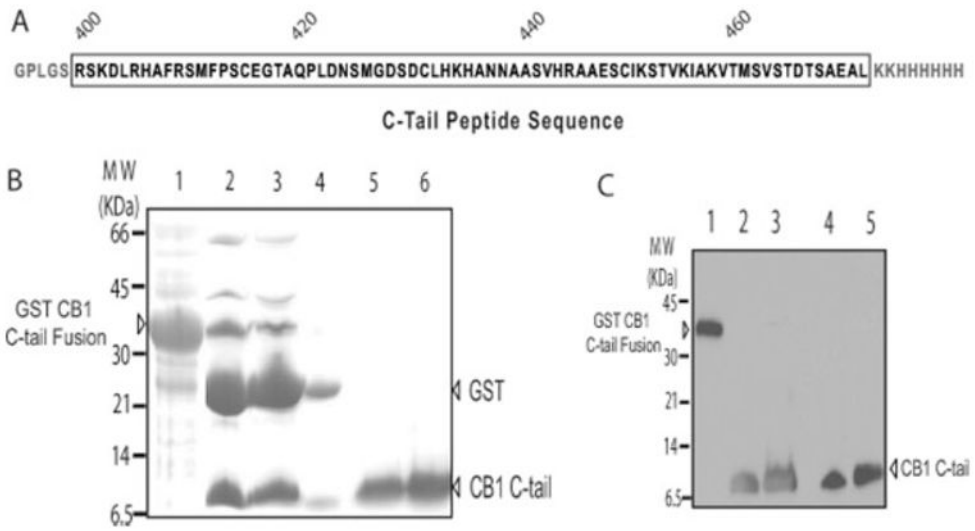

FIGURE 1.

CB1 C-tail peptide sequence and purification analysis. (A) Schematic representation of the sequence of the human CB1 C-tail peptide. The CB1 C-tail peptide sequence is given in the box. The five residues on the left are derived from the cloning vector after PreScission protease cleavage to remove GST, and the eight residues to the right of the box are two lysines and a His-tag as described in Materials and Methods. The amino acid numbers corresponding to the location in the sequence of the full-length wild-type human CB1 receptor are indicated. Note several studies of helix 8 employ the rat sequence that has an additional residue in the region.[12,13,30–32] (B) Tris-tricine SDS-PAGE analysis of the CB1 C-tail peptide expression and purification products. Lane 1: crude lysate; Lanes 2 and 3: on-column protease cleavage of the GST-fusion for 4 h and overnight, respectively; Lane 4: resin only after peptide elution to analyze for incomplete peptide removal; Lanes 5 and 6: C-tail peptide eluted after 4 h and overnight cleavage, respectively. (C) Western blot of the C-tail peptide after SDS-PAGE. Lane 1: crude lysate probed with antiserum against the His-tag; Lanes 2 and 3: peptide samples eluted after 4 h and overnight cleavage, respectively, and probed with antiserum against the His-tag; Lanes 4 and 5: peptide samples eluted after 4 h and overnight cleavage, respectively, probed with an antibody against the CB1 C-tail.

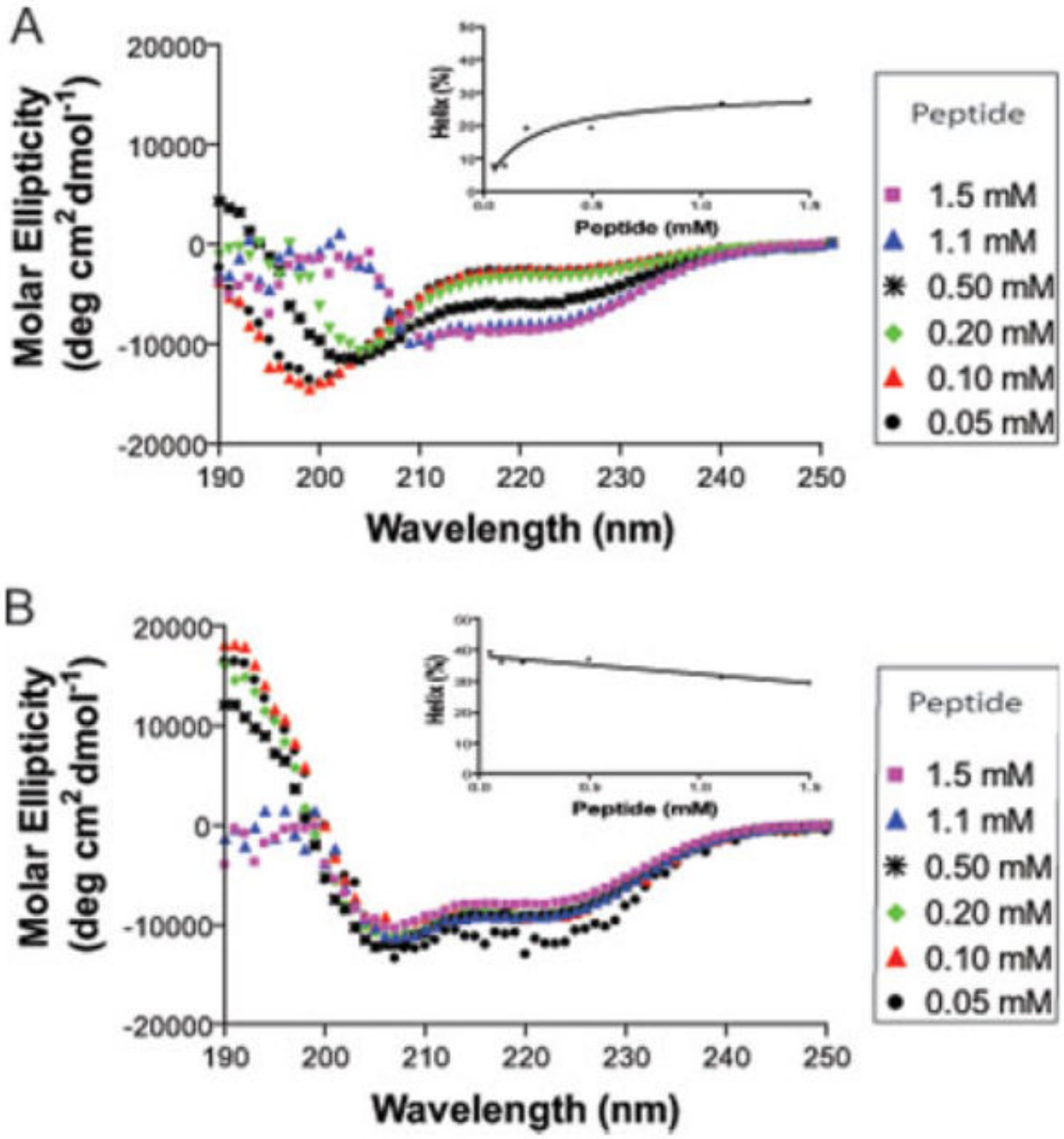

FIGURE 2.

Peptide concentration-dependent conformational transition of the CB1 C-tail peptide. CD spectra were recorded from 190 to 250 nm at various concentrations of the peptide in (A) 10 m*M* sodium phosphate, pH 7.2 or (B) 50 m*M* DPC. The insets show helicity as a function of increasing peptide concentration. Data represent the average of four experiments. The legends in the figure indicate the peptide concentrations examined.

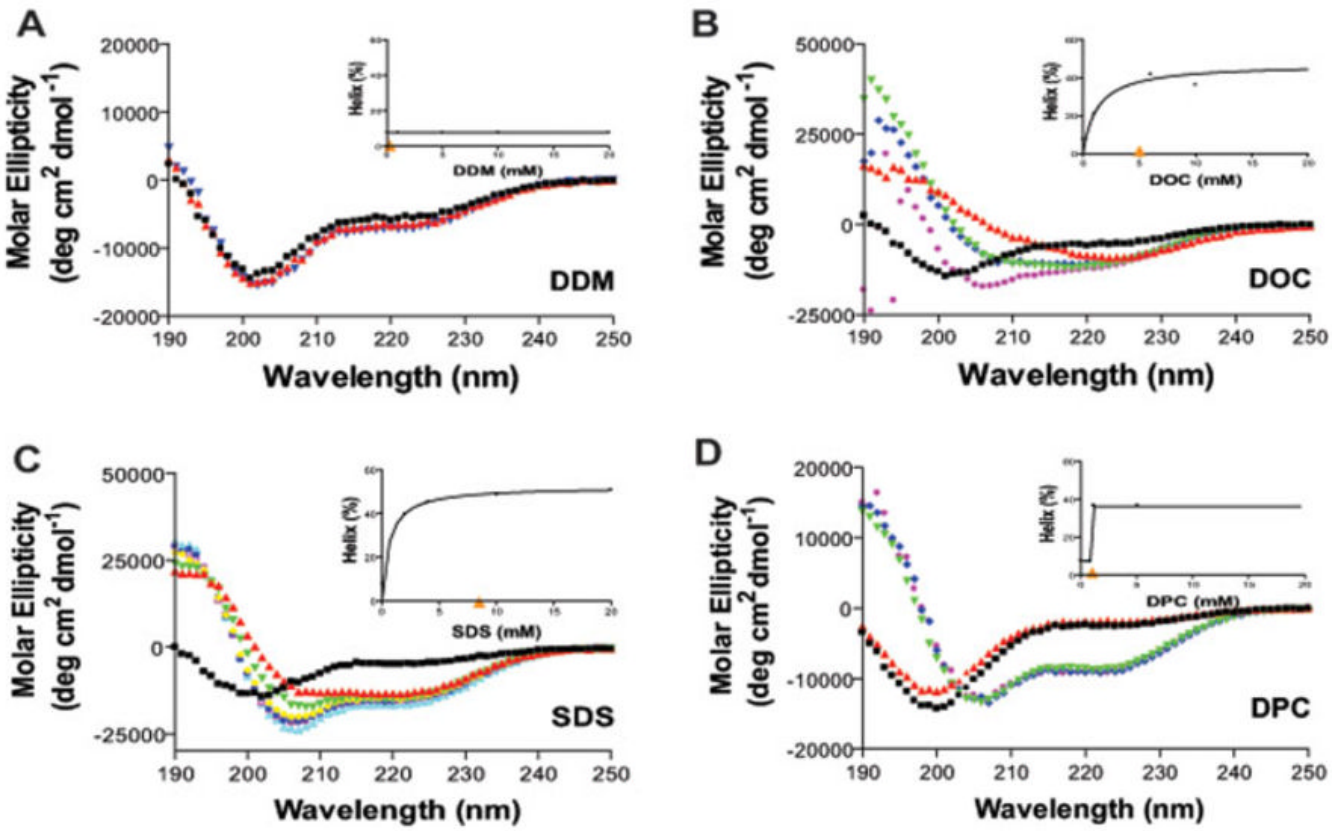

FIGURE 3.

CD spectra of the CB1 C-tail peptide in various detergents. The peptide concentration was 50 *μM*. (A) CD spectra of the peptide in the absence (■, in black) and presence of 1 m*M* (▲, in red) or 20 m*M* (▼;, in blue) DDM. (B) CD spectra of the peptide in the absence (■, in black) and presence 1 m*M* (▲, in red), 6 m*M* (▼;, in green), 10 m*M* (◆, in blue), or 30 m*M* (●, in red) DOC. (C) CD spectra of the peptide in the absence (■, in black) and presence of 2 m*M* (▲, in red), 4 m*M* (▼;, in green), 10 m*M* (◆, in yellow), 20 m*M* (●, in blue), 50 m*M* (□, in red), or 100 m*M* (△, in light blue) SDS. (D) CD spectra of the peptide in the absence (■, in black) and presence of 0.5 m*M* (▲, in red), 5 m*M* (▼;, in green), 50 m*M* (◆, in blue), or 100 m*M* (●, in red) DPC. Data represent the average of four experiments. The insets show helicity as a function of detergent concentration. The critical micelle concentration (CMC) of each detergent is indicated (▲, in orange) in the inset.

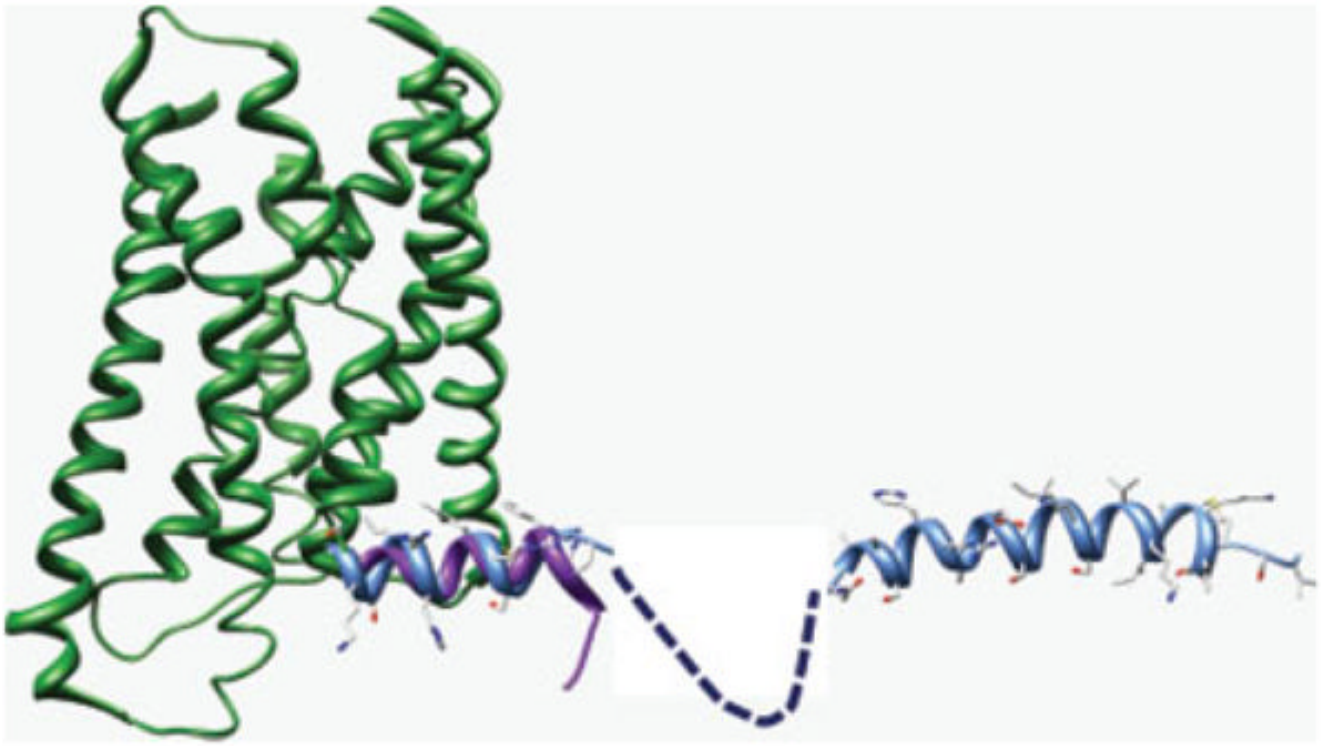

FIGURE 4.
Illustration of the superposition of the two α-helices as determined here for the human CB1 C-terminus onto the X-ray structure of rhodopsin, using the overlapping helix 8 observed for both systems. The 7 TM helices are colored green, with helix 8 in purple. The two CB1 helices are in blue, with the 28-residue gap between the helices denoted by a dashed line.

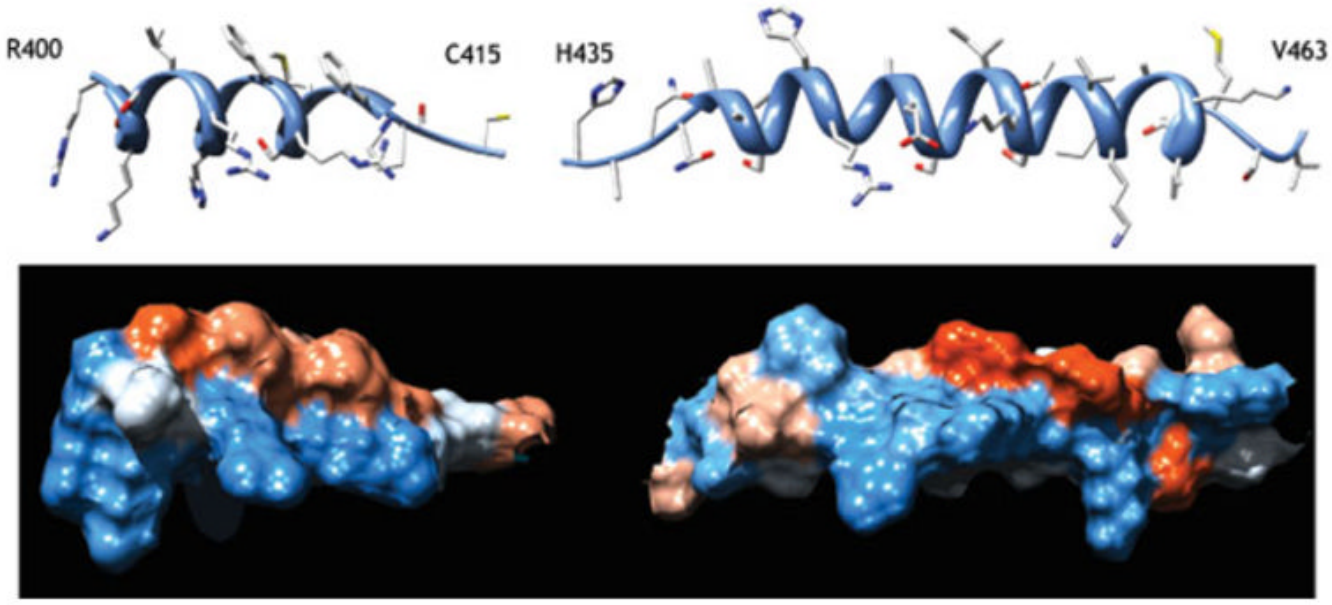

FIGURE 5.

Illustration of the amphipathic nature of the two α-helices observed for the C-terminus of the human CB1 receptor. The helical domains CB1 (401–412) (left) and CB1 (440–461) (right) are shown as ribbons (top) and as hydrophobic colored surfaces (bottom).

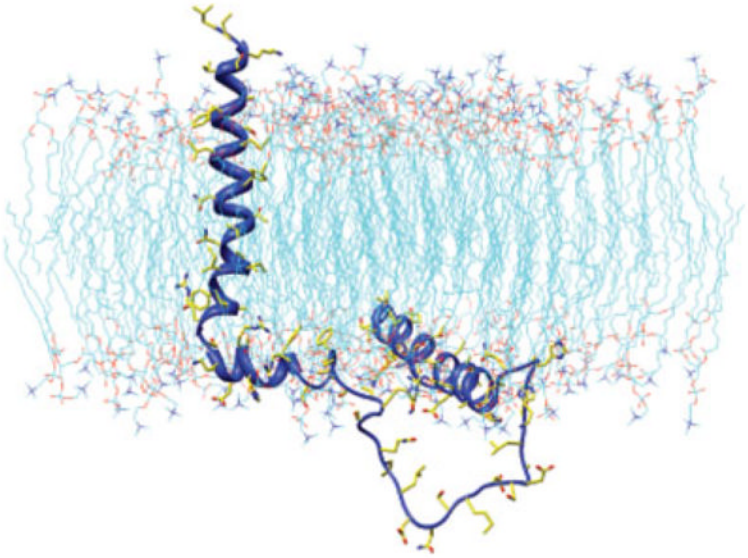

FIGURE 6.
Illustration of a snapshot (after 150 ps) from the MD trajectory of the TM7-C-terminus construct of the human CB1 receptor, CB1 (374–472). The receptor is illustrated as a ribbon (dark blue), with the side chain heavy atoms shown in yellow (carbon), blue (nitrogen), and red (oxygen). The lipids are shown with similar colors, but with blue carbons.